INL/EXT-06-11887

Advanced Test Reactor LEU Fuel Conversion Feasibility Study

(2006 Annual Report)

G.S. Chang
R.G. Ambrosek
M.A. Lillo

December 2006

The INL is a U.S. Department of Energy National Laboratory
operated by Battelle Energy Alliance

INL/EXT-06-11887

Advanced Test Reactor LEU Fuel Conversion Feasibility Study

(2006 Annual Report)

G.S. Chang
R.G. Ambrosek
M.A. Lillo

December 2006

Idaho National Laboratory
Idaho Falls, Idaho 83415

Prepared for the
U.S. Department of Energy
Office of Nuclear Energy
Under DOE Idaho Operations Office
Contract DE-AC07-05ID14517

ADVANCED TEST REACTOR

LEU FUEL CONVERSION FEASIBILITY STUDY

(2006 Annual Report)

G. S. Chang, R. G. Ambrosek (retired), and M. A. Lillo

Idaho National Laboratory
Idaho Falls, Idaho 83415 – United States

ABSTRACT

The Advanced Test Reactor (ATR) is a high power density and high neutron flux research reactor operating in the United States. Powered with highly enriched uranium (HEU), the ATR has a maximum thermal power rating of 250 MW_{th} with a maximum unperturbed thermal neutron flux rating of 1.0×10^{15} n/cm^2–s. Because of these operating parameters and large test volumes located in high flux areas, the ATR is an ideal candidate for assessing the feasibility of converting an HEU driven reactor to a low-enriched core. The present work investigates the necessary modifications and evaluates the subsequent operating effects of this conversion.

A detailed plate-by-plate MCNP ATR $1/8^{th}$ core model was developed and validated for a fuel cycle burnup comparison analysis. Using the current HEU U-235 enrichment of 93.0 % as a baseline, an analysis can be performed to determine the low-enriched uranium (LEU) density and U-235 enrichment required in the fuel meat to yield an equivalent K-eff between the HEU core and the LEU core versus effective full power days (EFPD). The MCNP ATR $1/8^{th}$ core model will be used to optimize the U-235 loading in the LEU core, such that the differences in K-eff and heat profile between the HEU and LEU core can be minimized for operation at 125 EFPD with a total core power of 115 MW.

The depletion methodology MCWO, was used to calculate K-eff versus EFPDs. The MCWO-calculated results for the LEU case demonstrated adequate excess reactivity such that the K-eff versus EFPDs plot is similar in shape to the reference ATR HEU case. The LEU core conversion feasibility study can also be used to optimize the U-235 content of each fuel plate, so that the relative radial fission heat flux profile is bounded by the reference ATR HEU case. The detailed radial, axial, and azimuthal heat flux profiles of the HEU and optimized LEU cases have been investigated. However, to demonstrate that the LEU core fuel cycle performance can meet the UFSAR safety requirements, additional studies will be necessary to evaluate and compare safety parameters such as void reactivity and Doppler coefficients, control components worth (outer shim control cylinders (OSCCs), safety rods and regulating rod), and shutdown margins between the HEU and LEU cores.

1. Introduction

The Advanced Test Reactor (ATR) at the Idaho National Laboratory (INL) is a high power density and high neutron flux research reactor operating in the United States. Powered with highly enriched uranium (HEU), the ATR has a maximum thermal power rating of 250 MW_{th} with a maximum unperturbed thermal neutron flux rating of 1.0×10^{15} n/cm^2–s. The conversion of nuclear test reactors currently fueled with HEU to operate with low-enriched uranium (LEU) is being addressed by the reduced enrichment for research and test reactors (RERTR) program. The ATR is a representative candidate for assessing the necessary modifications and evaluating the subsequent operating effects encountered when converting from HEU to LEU.

The scope of this task is to assess the feasibility of converting the ATR HEU fuel to LEU fuel while retaining all key functional and safety characteristics of the reactor. Using the current HEU U-235 enrichment of 93.0 % as a baseline, the study will determine the LEU uranium density required in the fuel meat to yield an equivalent K-eff between the HEU core and LEU core after 125 effective full power days (EFPDs) of operation with a total core power of 115 MW. A lobe power of 23 MW is assumed for each of the five lobes. Then, the U-235 loading determined to yield an equivalent K-eff will be used to predict radial, axial, and azimuthal power distributions. The heat rate distributions will also be evaluated for this core and used to predict the core performance as related to the current Upgraded Final Safety Analysis Report (UFSAR) and the associated Technical Safety Requirements (TSR's).

2. Advanced Test Reactor Description

The ATR was originally commissioned in 1967 with the primary mission of materials and fuels testing for the United States Naval Reactors Program. The ATR is a high power density and high neutron flux research reactor with large test volumes in high flux regions. General characteristics for the ATR are given in the "Users Handbook for the Advanced Test Reator." Powered with HEU, the ATR has a maximum thermal power rating of 250 MW_{th} with a maximum unperturbed thermal neutron flux rating of 1.0×10^{15} n/cm^2–s.

The ATR was designed to provide large-volume, high-flux test locations. The unique serpentine fuel arrangement provides nine high-intensity neutron flux traps and 68 additional irradiation positions inside the reactor core reflector tank, each of which can contain multiple experiments.

The ATR's unique control device design permits large power shifts among the nine flux traps. The ATR uses a combination of control cylinders or drums and neck shim rods. The control cylinders rotate hafnium plates toward and away from the core, and the shim rods, which withdraw vertically, are individually inserted or withdrawn to adjust power. Within bounds, the power level in each corner lobe of the reactor can be controlled independently.

The ATR has five lobes which are loosely coupled. These five lobes are identified as Northwest (NW), Northeast (NE), Center (C), Southwest (SW), and Southeast (SE). During full power operation, operators can maintain the desired lobe power by rotating the Outer Shim Control Cylinders (OSCC) and withdrawing/inserting the neck shim control rods. Each lobe can be viewed as a smaller, independent reactor, which means there are five reactors in the ATR. A Lobe-by-Lobe (LbyL) conversion strategy can be developed, minimizing the impacts to the important experiments within other lobes.

3. Validation of the Detailed Plate-by-Plate MCNP ATR Full Core Model

The ability to accurately predict K-eff and fission power distribution within the 19 fuel plates using the MCNP model is essential to the ATR LEU core conversion design. The purpose of this section is to discuss the difference in K-eff calculated by MCNP (Case-1) and PDQ (Case-2)[1] models with respect to the Cycle 134A (Case-3) ATR SUrveillance DAta System (ASUDAS)[2] data. The ATR Cycle 134A core configuration was modeled using MCNP and PDQ, then input parameters were adjusted to reflect the as-run Cycle 134A initial critical conditions given in The PDQ calculations were performed using the PDQWS[3] computer code. Because the PDQ core model uses a discrete X-Y mesh to divide the cells, the balanced outer shim position was modeled at 40.1°, which was the closest available position to the ASUDAS value of 39.2°. The MCNP and PDQWS calculated results and ASUDAS data are tabulated in Table 2.

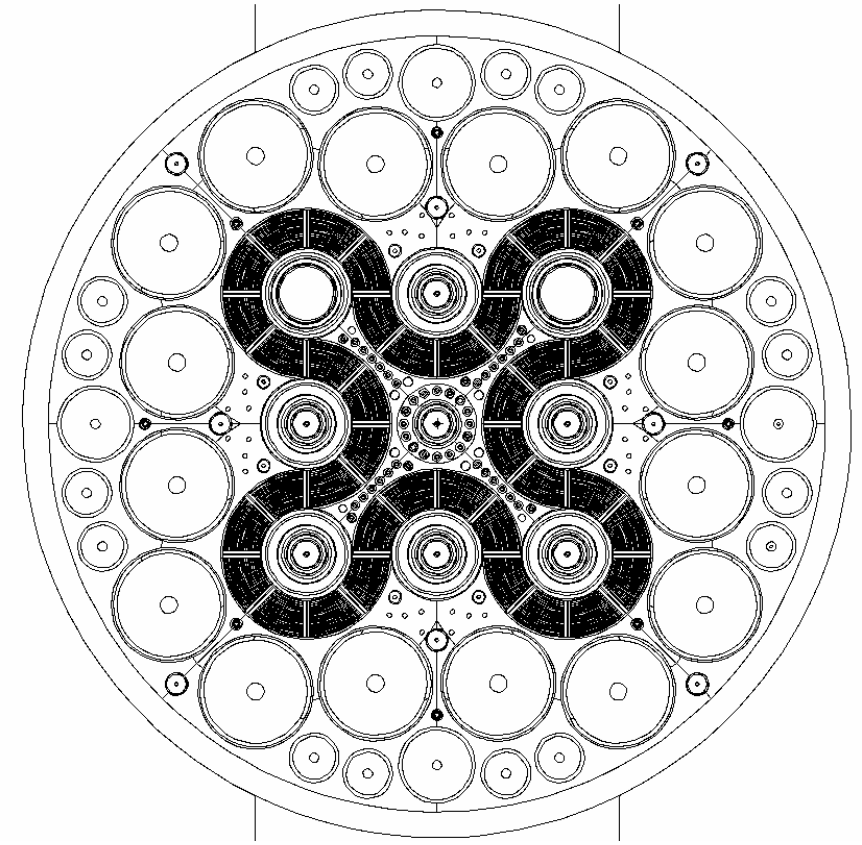

Figure 1. ATR MCNP full core model with 19 fuel plates per FE.

Table 1. The detailed plate-by-plate MCNP ATR full core model was used to generate **Error! Reference source not found.**. The 40 fuel elements (FE) are explicitly modeled with 19 plates per FE.

The PDQ calculations were performed using the PDQWS[3] computer code. Because the PDQ core model uses a discrete X-Y mesh to divide the cells, the balanced outer shim position was modeled at 40.1°, which was the closest available position to the ASUDAS value of 39.2°. The MCNP and PDQWS calculated results and ASUDAS data are tabulated in Table 2.

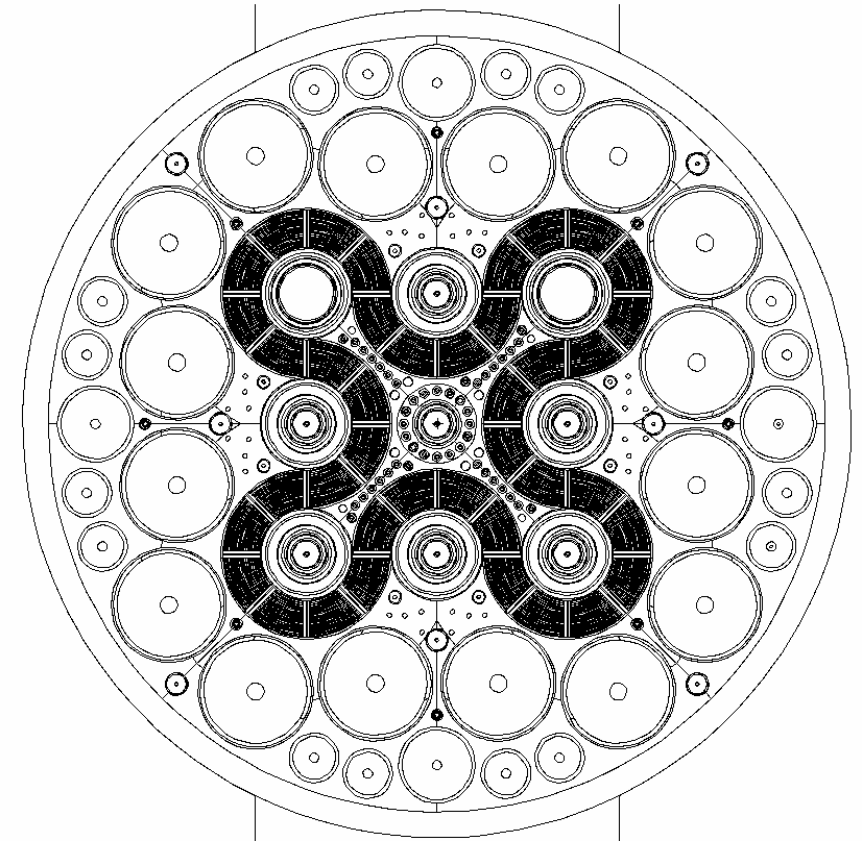

Figure 1. ATR MCNP full core model with 19 fuel plates per FE.

Table 1. ATR Cycle 134A ASUDAS (as-run) initial critical conditions.

Parameter	Case-3
Balanced OSCC Position	39.2˚
K-eff	1.00 (Critical)
Neck Shim Positions: NW 1-6, NE 1-6, SW 1-3 & 5-6, SE 1-3 & 5-6	All inserted

Table 2. Initial critical conditions for ATR Cycle 134A (MCNP, PDQWS, and ASUDAS).

Case	Balanced OSCC	K-eff
Case-1 (MCNP)	39.2°	1.0011
Case-2 (PDQWS)	40.1°	0.9886
Case-3 (ASUDAS)	39.2˚	1.0000

Case-1 compared to Case-3 Δ K-eff (ASUDAS – MCNP) = 1.0000 – 1.0011 = -0.0011

Case-2 compared to Case-3 Δ K-eff (ASUDAS – PDQWS) = 1.0000 – 0.9886 = 0.0114

From these calculations, it was concluded that (a) the bias of PDQ ATR model with respect to ASUDAS data is 0.0114, while (b) the bias of the ATR full core MCNP model with respect to ASUDAS data is -0.0011, and (c) the ATR full core MCNP K-eff calculation and ASUDAS measured data are in good agreement.

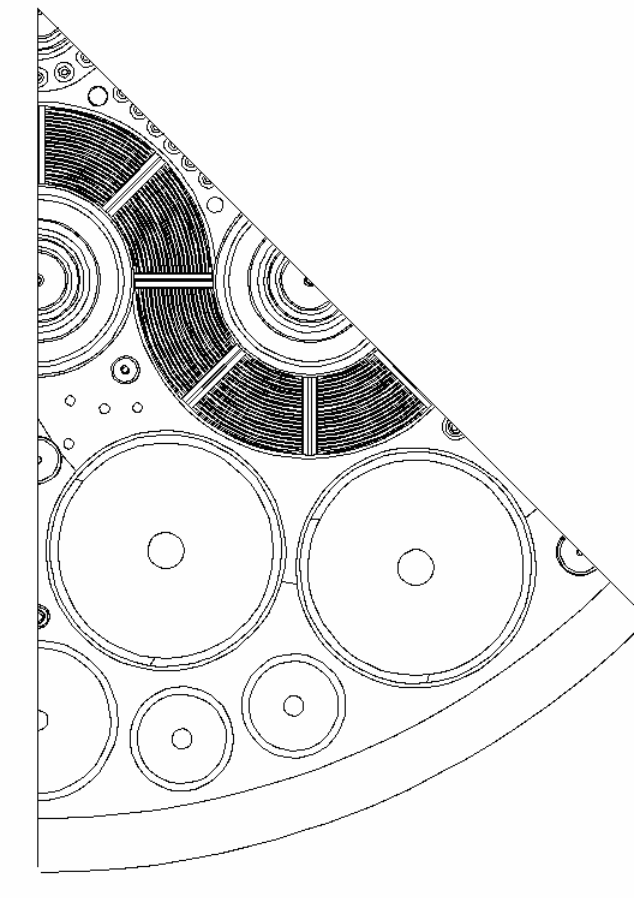

Figure 2. ATR SE-lobe 1/8th core MCNP model (FE 16-20).

4. Plate-by-Plate ATR 1/8th Core Model for Fuel Burnup Analysis

A detailed plate-by-plate MCNP ATR 1/8th core model as shown in **Error! Reference source not found.** was derived from the validated MCNP ATR full core model for the fuel cycle burnup analysis. This model is used to optimize the U-235 loading in the LEU core by minimizing the K-eff differences with respect to the HEU core after 125 EFPDs of operation at total core power of 115 MW (23 MW per lobe).

5. MCWO – Fuel Burnup Analysis Tool

The fuel burnup analysis tool used in this study consists of a BASH script file that links together the two FORTRAN data processing programs, m2o.f[4] and o2m.f[4]. This burnup methodology couples the Monte Carlo transport code MCNP[5,6] with the radioactive decay and burnup code ORIGEN2[7], and is known as Monte Carlo with ORIGEN2, or MCWO[4,8].

The MCWO methodology produces criticality and burnup data based on various material feed/removal specifications, core power(s), and irradiation time intervals. MCWO processes user-specified input for geometry, initial material compositions, feed/removal specifications, and other problem-specific parameters. The MCWO methodology uses MCNP-calculated one-group microscopic cross sections and fluxes as input to a series of ORIGEN2 burnup calculations.

ORIGEN2 depletes/activates materials and generates isotopic compositions for subsequent MCNP calculations. MCWO performs one MCNP and one or more ORIGEN2 calculations for each user-specified time step. Due to the highly time-dependent nature of the physics parameters and material compositions of the modeled reactor system, the MCWO-calculated results are typically more accurate if long irradiation cycles are broken up into smaller intervals. It should be noted that an increase in the number of ORIGEN2 calculation steps does not significantly impact the overall MCWO execution time because MCNP dominates the MCWO execution time.

For each MCNP calculation step, MCNP updates the fission power distribution and burnup-dependent cross sections for each fuel plate then transfers data to ORIGEN2 for cell-wise depletion calculations. The MCNP-generated reaction rates are integrated over the continuous-energy nuclear data and the space within the region.

6. Neutronics Evaluation of HEU and Un-Optimized LEU

MCWO was used to perform an evaluation of the fuel cycle performance versus the EFPDs for: Case-A1, ATR reference HEU, 20 mil thick fuel meat, 1075 g U-235, no B-10 loading; Case-A2, ATR reference HEU, 20 mil thick fuel meat, 1075 g U-235, 0.66 g B-10 loading; Case-B1, Foil type LEU, 10 mil thick U-10Mo fuel meat, 1204.2 g U-235; Case-C1, Foil type LEU, 10 mil thick U-7Mo fuel meat, 1263.1 g U-235. The analysis assumed that each nominal operating cycle was 50 EFPDs followed immediately by a seven day outage. Each 50 EFPD cycle was subdivided into 5 EFPD time step intervals. The OSCC positions were set to 96°. The resultant MCNP-calculated tallies were normalized to a south lobe source power of 23 MW.

6.1 Comparison of K-eff Versus EFPDs

The MCWO-calculated results of the bias adjusted K-eff versus EFPDs for Case-A1 and -A2 demonstrates that the ATR HEU fuel provides adequate excess reactivity (for K-eff larger than one) for about 120 EFPDs of reactor power operation.

The MCWO-calculated results of the bias adjusted K-eff versus EFPDs for Case-B1 and -C1 demonstrates that the LEU foil fuel types also provide adequate excess reactivity (for K-eff larger than one) for about 120 EFPDs of reactor power operation. The fuel densities for Case-B1 and -C1 were 16.88 g/cc and 17.45 g/cc, respectively and the U-235 contents were 1204.2 g and 1263.1 g, respectively.

The MCWO-calculated K-eff for HEU Case-A1 and -A2, and LEU Case-B1 and -C1 are plotted in Figure 3. Please note that at the beginning of cycle (BOC) for each of the three nominal operating cycles modeled, the initial Xe poison was set to zero or decayed to a very small value during the 7 day shutdown time, thus causing a jump increase in K-eff.

6.2 Comparison of Radial Fission Power Profiles at BOC

For the beginning of the first cycle, the relative radial plate fission power heat flux was calculated using the MCWO methodology. Results for Case-A1, -B1, and -C1 are plotted in Figure 4. It is apparent that when compared to Case-A1, Case-B1 and -C1 yield significantly higher heat fluxes at the inner/outer plates.

In FE-18, the respective peak heat fluxes local-to-average-ratios (L2ARs) for Case-A1, -B1, and -C1 was determined to be 1.30, 1.59, and 1.63, respectively. The peak flux occurred in plate 19 for all three cases. HEU Case-A2 has B-10 loading in the 4 inner/outer fuel plates (plates 1-4 and 16-19). The B-10 is a burnable poison which flattens the relative heat flux in the inner/outer plates to a peak value of about 1.22. Case-B1 and -C1 do not have any burnable absorber, therefore the peak relative heat flux ratio is approximately 1.63. From these results, it was established that the LEU fuels analyzed in Case-B1 and -C1 have rather high L2AR heat fluxes at both the inner/outer plates.

For HEU reference Case-A1, the lower L2AR at the inner/outer plates is due to the lower U-235 densities within those 4 inner/outer plates. For the HEU reference Case-A2, the 4 inner/outer plates are loaded with 0.66 g of B-10, a burnable poison, which causes the heat flux profile to flatten even more when compared with HEU Case-A1. The HEU Case-A2 fuel plate specifications are given in **Error! Reference source not found.**.

To reduce the LEU heat flux L2AR, the U-235 contents and thickness of the inner/outer plates was evaluated and optimized. The LEU fuel loading was optimized such that the L2AR at the 4 inner/outer

plates is bounded by reference HEU Case-A2. The optimization was achieved by 1) varying the U-235 enrichment and 2) reducing the fuel meat thickness as well as loading the inner/outer plates with 0.68 g of B-10.

Table 3. Specifications for a standard ATR HEU FE with B-10 in the 4 inner/outer fuel plates.

HEU Plate	Plate Volume (cc)	U-235 Mass (g)	B-10 Mass (g)	U-235 Density (g/cc)
Plate-1	23.69	24.3	0.063	1.026
Plate-2	29.54	29.1	0.078	0.985
Plate-3	31.12	38.7	0.044	1.243
Plate-4	32.70	40.4	0.045	1.235
Plate-5	34.29	52.1	--	1.520
Plate-6	35.87	54.6	--	1.522
Plate-7	37.45	57.0	--	1.522
Plate-8	39.03	59.4	--	1.522
Plate-9	40.61	61.8	--	1.522
Plate-10	42.19	64.2	--	1.522
Plate-11	43.78	66.6	--	1.521
Plate-12	45.36	69.0	--	1.521
Plate-13	46.94	71.4	--	1.521
Plate-14	48.52	73.8	--	1.521
Plate-15	50.10	76.3	--	1.523
Plate-16	51.69	64.0	0.071	1.238
Plate-17	53.27	65.9	0.073	1.237
Plate-18	54.22	53.8	0.143	0.992
Plate-19	52.64	52.6	0.143	0.999
Total	792.99	1075	0.66	--

6.3 Azimuthal and Axial Fission Power Profiles

To investigate the azimuthal fission power L2AR profiles, plates 2-19 were subdivided into 10 azimuthal regions and plate 1 was subdivided into 8 azimuthal regions. To investigate the axial fission power L2AR profiles, the 48 inch fuel plate was axially subdivided into 32 equal regions.
The MCNP-calculated results indicate that all HEU and LEU cases have similar azimuthal and axial fission power profiles as shown in Figure 5 and Figure 6. Therefore the average azimuthal and axial fission power profiles can and will be used for the fuel cycle burnup and thermal performance analysis.

7. Evaluation of HEU and Optimized LEU Fuel Cycle Performance

Based on the results of previously discussed comparisons, a study was performed to optimize the radial power profile of the LEU fuel plates such that the profile closely matches that of the HEU reference Case-A2. The optimization was based upon a comparison of the calculated radial power profile for various LEU fuel loading schemes. The fuel loading schemes included varying parameters such as fuel meat thickness and U-235 enrichment within the U10-Mo and U7-Mo LEU fuel types.

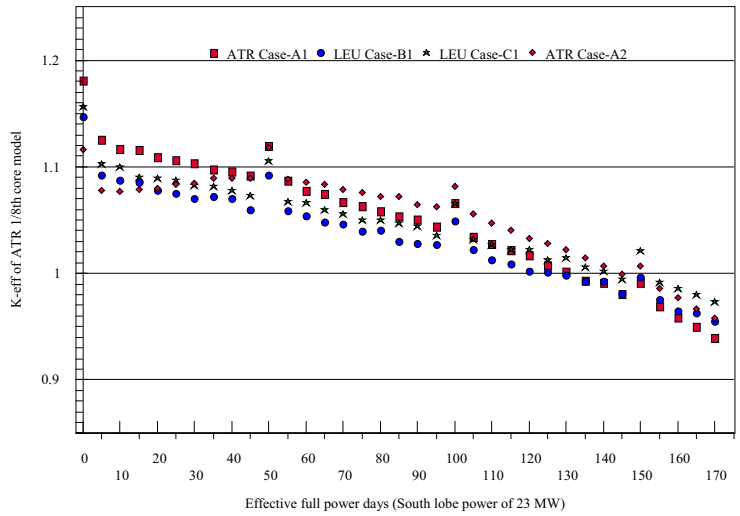

Figure 3. K-eff vs. EFPDs for ATR HEU Case-A1 and -A2, and LEU Case-B1 and -C1.

7.1 Optimized LEU Radial Fission Power Profile at BOC

Table 4 summarizes the parameter variations that resulted in the flattest radial fission heat profile while still maintaining sufficient reactivity within the LEU core. Not surprisingly, the optimal LEU fuel loading is similar to the HEU reference case. The optimal LEU fuel loading has thinner plates and lower enrichments at the inner/outer plate positions. It is apparent that further LEU fuel loading optimization studies should be performed. For the purposes of determining the feasibility of HEU to LEU conversion, however, the present study demonstrates a satisfactory loading scheme to achieve acceptable reactivity for three nominal 50 EFPD fuel cycles as well as maintain the radial heat flux L2AR profile.

The MCWO methodology was used to calculate the relative radial plate fission power heat flux for the optimized LEU cases for the beginning of the first cycle. In FE-18, the respective peak heat fluxes L2AR for Case-A2, -B2, and -C2 was determined to be 1.22, 1.12, and 1.13, respecively. Results for Case-A2, -B2, and -C2 are plotted in Figure 7. This plot demonstrates that Case-B2 and -C2 yield very similar radial L2AR profiles as compared to Case-A2.

For the variable U-235 enrichment, the MCWO-calculated radial L2AR profiles of Case-B3 and -C3 as compared to Case-A2 are plotted in Figure 8. This plot demonstrates that Case-B3 and -C3 yield very similar radial L2AR profiles as compared to Case-A2. In FE-18, the respective peak heat fluxes L2AR for Case-A2, -B3, and -C3 are 1.22, 1.12, and 1.12, respectively.

7.2 Optimized LEU K-eff versus EFPDs

Using the optimized LEU fuel loadings, the MCWO-calculated K-eff for LEU Case-B2 and -C2 as a function of EFPDs as compared to the HEU reference Case-A2 is shown in Figure 9. For the LEU U-235 enrichment variation, the MCWO-calculated K-eff for LEU Case-B3 and -C3 as a function of EFPDs as compared to the HEU Case-A2 is shown in Figure 10. Please note that the LEU fuels contain 80.3 wt% U-238, which can be transmuted to Pu-239. Although the LEU cases have a lower K-eff at the BOC when compared with HEU Case-A2, the LEU cases sustain operation for more EFPDs than HEU Case-A2 (at least 140 EFPDs).

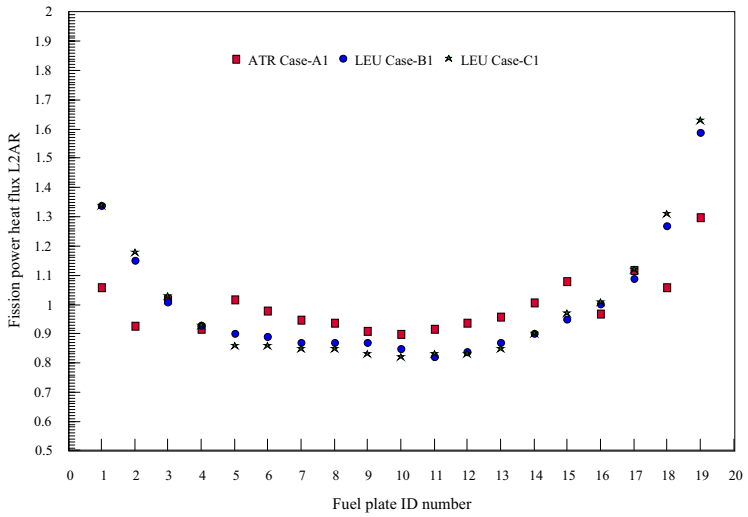

Figure 4. Radial fission power heat flux L2AR for ATR HEU Case-A1, LEU Case-B1 and -C1.

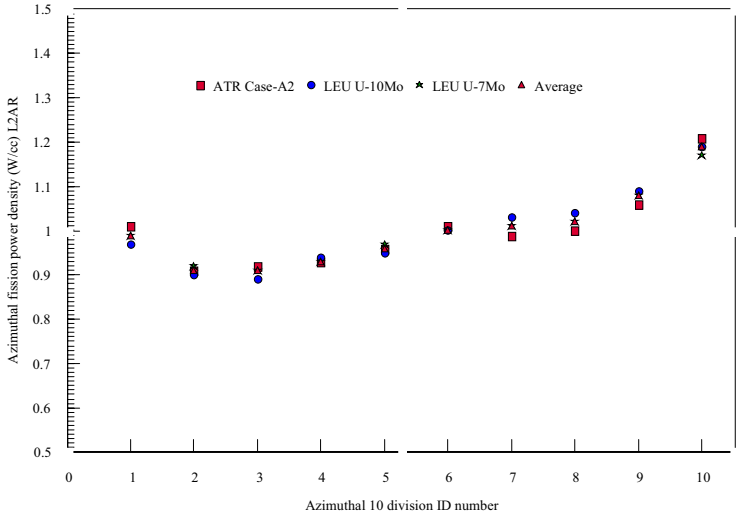

Figure 5. FE-18 Azimuthal distribution of fission power density L2AR.

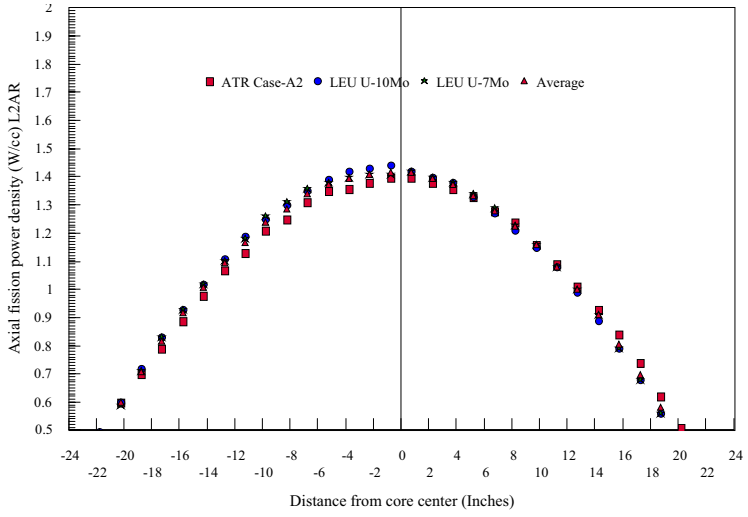

Figure 6. FE-18 Axial Distribution of fission power density L2AR.

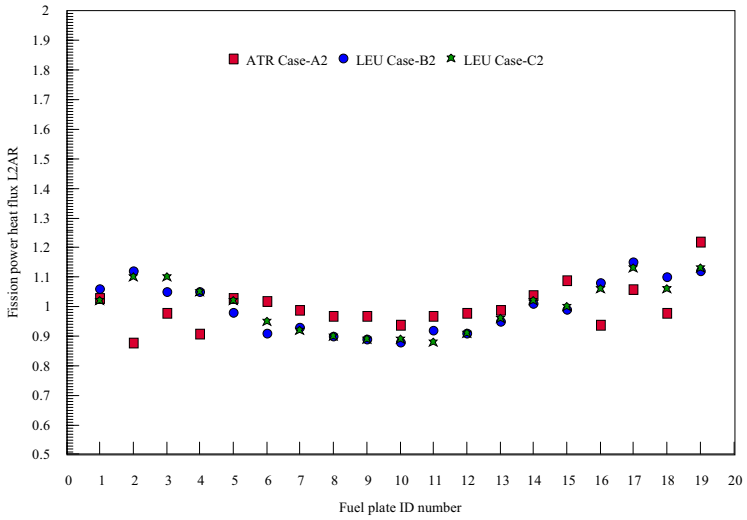

Figure 7. Fission power heat flux L2AR radial profiles for HEU Case-A2, LEU Case-B2 and -C2.

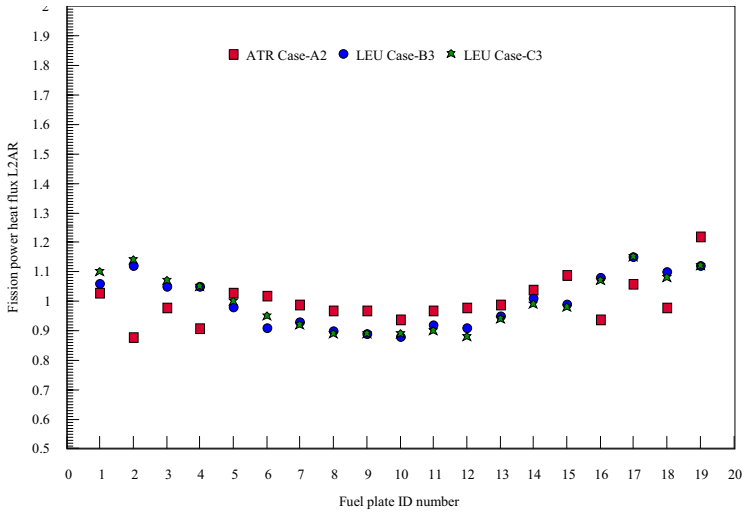

Figure 8. Fission power heat flux L2AR radial profiles for HEU Case-A2, LEU Case-B3 and -C3.

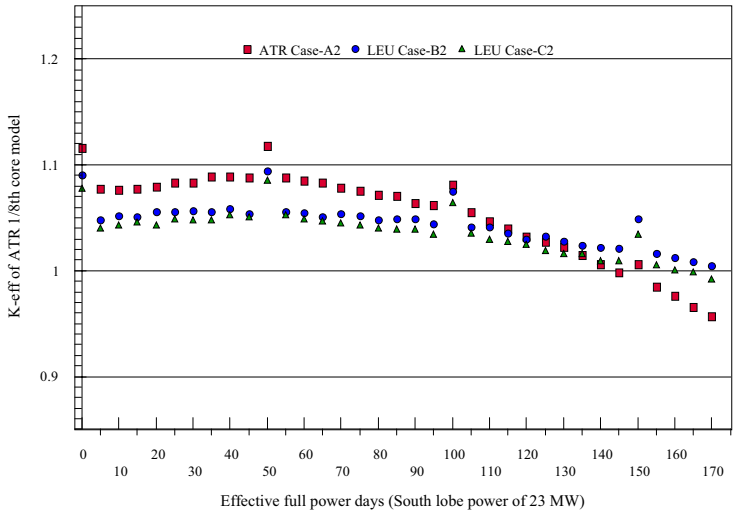

Figure 9. MCWO-calculated K-eff versus EFPDs for HEU Case-A2, LEU Case-B2 and -C2.

Table 4. Parameter variations used for radial power profile comparison studies.

Plate #	Case-B2 Fixed U-235 (wt%)	Case-B2 Vary thickness (inches)	Case-B3 Vary U-235 (wt%)	Case-B3 Fixed thickness (inches)	Case-C2 Fixed U-235 (wt%)	Case-C2 Vary thickness (inches)	Case-C3 Vary U-235 (wt%)	Case-C3 Fixed thickness (inches)
1	19.70%	0.0096	11.82%	0.016	19.70%	0.0078	11.82%	0.013
2	19.70%	0.0128	15.76%	0.016	19.70%	0.0104	15.76%	0.013
3	19.70%	0.0144	17.73%	0.016	19.70%	0.0117	17.73%	0.013
4	19.70%	0.0160	19.70%	0.016	19.70%	0.013	19.70%	0.013
5	19.70%	0.0160	19.70%	0.016	19.70%	0.013	19.70%	0.013
6	19.70%	0.0160	19.70%	0.016	19.70%	0.013	19.70%	0.013
7	19.70%	0.0160	19.70%	0.016	19.70%	0.013	19.70%	0.013
8	19.70%	0.0160	19.70%	0.016	19.70%	0.013	19.70%	0.013
9	19.70%	0.0160	19.70%	0.016	19.70%	0.013	19.70%	0.013
10	19.70%	0.0160	19.70%	0.016	19.70%	0.013	19.70%	0.013
11	19.70%	0.0160	19.70%	0.016	19.70%	0.013	19.70%	0.013
12	19.70%	0.0160	19.70%	0.016	19.70%	0.013	19.70%	0.013
13	19.70%	0.0160	19.70%	0.016	19.70%	0.013	19.70%	0.013
14	19.70%	0.0160	19.70%	0.016	19.70%	0.013	19.70%	0.013
15	19.70%	0.0144	17.73%	0.016	19.70%	0.0117	17.73%	0.013
16	19.70%	0.0144	17.73%	0.016	19.70%	0.0117	17.73%	0.013
17	19.70%	0.0128	15.76%	0.016	19.70%	0.0104	15.76%	0.013
18	19.70%	0.0096	11.82%	0.016	19.70%	0.0078	11.82%	0.013
19	19.70%	0.0074	9.09%	0.016	19.70%	0.0066	10.03%	0.013

Note: Case-B2 and -B3, U10-Mo has fixed U density of 16.88 g/cc, Case-C2 and -C3, U7-Mo has fixed U density of 17.45 g/cc.

These studies indicate that the LEU radial L2AR profiles can achieve flattened profiles bounded by HEU reference Case-A2 by either varying fuel meat thickness or reducing U-235 enrichment within the inner/outer 4 plates. However, the fission power density (W/cm^3) L2AR profiles for the LEU cases with varied fuel meat thickness produced larger peaks within the inner/outer plates (see Figure 11). This peaking will result in large, undesirable fission density (fissions/cc) accumulation for a given discharge burnup. As a result, the varied U-235 enrichment is the preferred approach to achieve the optimal fuel cycle performance.

8. HEU and LEU Core Thermal-Hydraulic Evaluation

This preliminary evaluation of the radial heat generation rates indicates that the outer fuel plates have heat rates that are considerably higher than the heat rates for the HEU plates containing boron. This indicates that the fuel, as analyzed, would not allow operation within the current authorization basis which is based on the UFSAR and radial power distributions with the boronated HEU in the identified plates. As noted previously, adjustments to uranium loading or addition of neutron poisons appear to be possible due to the excess reactivity as compared to the HEU fuel loading. Further evaluations will be necessary to ascertain if the current operational envelope can be maintained, since the operation is based on a point power concept and the radial, axial, and azimuthal peaking need to be combined to obtain a point power.

A thermal-hydraulic evaluation will compare the HEU and LEU results for radial, axial and azimuthal heating profiles, and magnitude when the heating rates are available. Differences will then be identified,

providing a preliminary assessment for demonstrating that the UFSAR provides a safe operating envelop for the LEU fuel. The results will then be documented and recommendations provided for minimizing the differences.

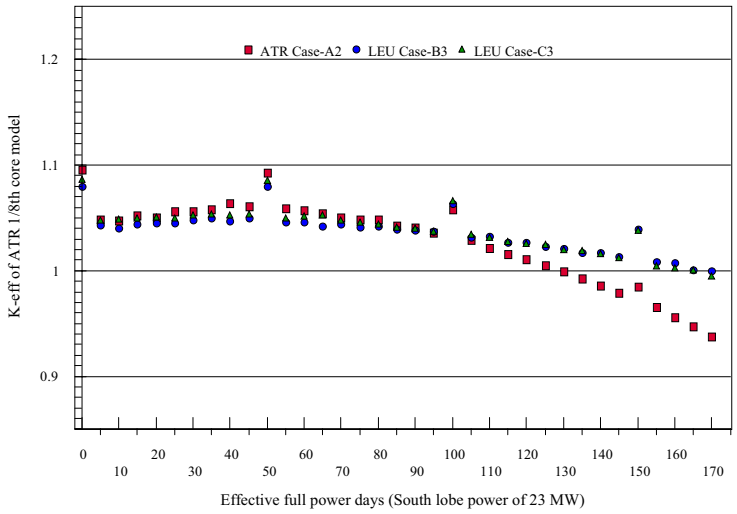

Figure 10. MCWO-calculated K-eff versus EFPDs for HEU Case-A2, LEU Case-B3 and -C3.

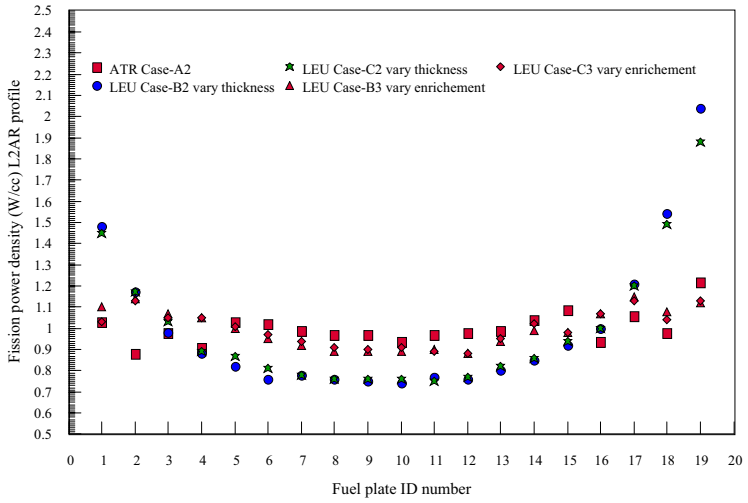

Figure 11. Fission power density L2AR radial profiles for HEU Case-A2 and optimized LEU cases.

9. Conclusions and Recommendations

For this study, the detailed plate-by-plate MCNP ATR 1/8th core model was developed and validated. This study also demonstrated that the 1/8th core model adequately represents the whole ATR core model for neutronics burnup analysis characterization. The detailed plate-by-plate MCNP ATR 1/8th core model used in this study is handles complex spectral transitions at the boundaries between the plates in a straightforward manner.

The MCWO-calculated K-eff versus EFPDs results indicate that both LEU Case-B3 and -C3 provide excess reactivity versus burnup while providing fission heat profiles similar to HEU Case-A2. The LEU core conversion designer will be able to optimize the U-235 fuel loading so that the K-eff and relative

radial fission heat flux profile are similar to Case-A2, the current HEU fuel type. To achieve the flattened heat flux profile, the LEU core designer can either use the dispersed type LEU fuel or reduce the U-235 enrichment at the inner and outer plates. As a result, it has been concluded that LEU core conversion for the ATR is feasible.

The LEU core designer can use the detailed plate-by-plate MCNP ATR 1/8th core model to optimize the U-235 loading by either minimizing K-eff differences with respect to the HEU core during the 115 EFPDs of operation at a total core power of 115 MW (23 MW per lobe), or by reducing the higher L2AR of heat flux at the inner/outer plates. However, to demonstrate that the LEU core fuel cycle performance can meet the UFSAR safety requirement, a further study will be necessary in order to investigate the detailed radial, axial, and azimuthal heat flux profile variations versus EFPDs.

10. References

[1] Roth, P. A., 2004a, letter to J. D. Abrashoff, PAR-17-04, revision 1, "Startup Outer Shim Prediction for ATR Cycle 134A-1, Revision 1," December 20, 2004.

[2] ASUDAS report from DAC Hourly Control History for Cycle 134A-1/A-2 End of Cycle; provided by email from D. V. Thomas to M. A. Lillo, July 11, 2005.

[3] Cook W. C., Smith A. C., "ATR CSAP Package on the Workstation Version 1," PG-T-96-002, May, 1996.

[4] G. S. Chang, "MCWO - LINKING MCNP AND ORIGEN2 FOR FUEL BURNUP ANALYSIS," Proceedings of 'The Monte Carlo Method: Versatility Unbounded In A Dynamic Computing World,' Chattanooga, Tennessee, April 17–21, 2005, on CD-ROM, American Nuclear Society, LaGrange Park, IL (2005).

[5] Tim Goorley, Jeff Bull, Forrest Brown, et. al., "Release of MCNP5_RSICC_1.30," MCNP Monte Carlo Team X-5, LA-UR-04-4519, Los Alamos National Laboratory, November 2004.

[6] X-5 Monte Carlo Team, "MCNP—A General Monte Carlo N-Particle Transport Code, Version 5," Volume I (LA-UR-03-1987) and Volume II (LA-CP-0245), Los Alamos National Laboratory April 24, 2003 (Revised 6/30/2004).

[7] G. Croff, "ORIGEN2: A Versatile Computer Code for Calculating the Nuclide Compositions and Characteristics of Nuclear Materials, Nuclear Technology," Vol. 62, pp. 335-352, 1983.

[8] G. S. Chang and J. M. Ryskamp, "Depletion Analysis of Mixed Oxide Fuel Pins in Light Water Reactors and the Advanced Test Reactor," Nucl. Technol., Vol. 129, No. 3, p. 326-337 (2000).